

# Spin decoherence of a heavy hole coupled to nuclear spins in a quantum dot

Jan Fischer,<sup>1</sup> W. A. Coish,<sup>1,2</sup> D. V. Bulaev,<sup>1,3</sup> and Daniel Loss<sup>1</sup>

<sup>1</sup>*Department of Physics, University of Basel, Klingelbergstrasse 82, 4056 Basel, Switzerland*

<sup>2</sup>*Institute for Quantum Computing and Department of Physics and Astronomy,  
University of Waterloo, 200 University Ave. W., Waterloo, ON, N2L 3G1, Canada*

<sup>3</sup>*Institute of Solid State Physics, Russian Academy of Sciences, 142432 Chernogolovka, Moscow District, Russia*

(Dated: February 24, 2019)

We theoretically study the interaction of a heavy hole with nuclear spins in a quasi-two-dimensional III-V semiconductor quantum dot and the resulting dephasing of heavy-hole spin states. It has frequently been stated in the literature that heavy holes have a negligible interaction with nuclear spins. We show that this is not the case. In contrast, the interaction can be rather strong and will be the dominant source of decoherence in some cases. We also show that the form of the interaction is Ising-like, resulting in unique and interesting decoherence properties, which might provide a crucial advantage to using dot-confined hole spins for quantum information processing, as compared to electron spins.

PACS numbers: 03.65.Yz, 72.25.Rb, 73.21.La, 31.30.Gs

The spin of a quantum-dot-confined electron is considered a major candidate for the realization of solid-state-based quantum bits [1], the basic building blocks for quantum information processing devices and, eventually, for a quantum computer [2]. One of the main obstacles to building these devices is the decay of spin coherence. The ultimate limit to the coherence time for electron spins in most quantum dots at low temperatures is set by the hyperfine interaction with nuclei in the host material [3, 4, 5]. If no special effort is made to control this environment, the associated coherence times are quite short, typically on the order of nanoseconds [4, 5, 6].

Very recently, several experiments have shown initialization and readout of single hole spins [7], a prerequisite for coherence-time measurements. Hole-spin coherence times in III-V semiconductor quantum dots are anticipated to be much longer than electron-spin coherence times due to a weak hyperfine coupling relative to conduction-band electrons [8]. In the present work, we show that, in contrast, the coupling of a heavy hole (HH) to the nuclear spins in a quantum dot can be rather strong, potentially leading to coherence times that are comparable to those for electrons. However, in the quasi-two-dimensional (Q2D) limit, this interaction takes-on a simple Ising-like form,

$$H = \sum_k A_k^h s_z I_k^z, \quad (1)$$

where  $A_k^h$  is the coupling of the HH to the  $k^{\text{th}}$  nucleus,  $s_z$  is the hole pseudospin- $\frac{1}{2}$  operator, and  $I_k^z$  is the  $z$ -component of the  $k^{\text{th}}$  nuclear-spin operator  $\mathbf{I}_k$ . We find that the form of this effective Hamiltonian may allow for an extension of hole-spin coherence times well beyond those for electrons, even at low magnetic fields.

For a relativistic electron in the electromagnetic field of a nucleus with non-zero spin at position  $\mathbf{R}_k$ , there are three terms that couple the electron spin and orbital an-

gular momentum to the spin of the nucleus: the Fermi contact hyperfine interaction ( $h_1^k$ ), a dipole-dipole-like interaction (the anisotropic hyperfine interaction,  $h_2^k$ ), and the coupling of electron orbital angular momentum to the nuclear spin ( $h_3^k$ ). Setting  $\hbar = 1$ , these interactions are described by the following Hamiltonians [9]:

$$h_1^k = \frac{\mu_0}{4\pi} \frac{8\pi}{3} \gamma_S \gamma_{j_k} \delta(\mathbf{r}_k) \mathbf{S} \cdot \mathbf{I}_k, \quad (2)$$

$$h_2^k = \frac{\mu_0}{4\pi} \gamma_S \gamma_{j_k} \frac{3(\mathbf{n}_k \cdot \mathbf{S})(\mathbf{n}_k \cdot \mathbf{I}_k) - \mathbf{S} \cdot \mathbf{I}_k}{r_k^3(1 + d/r_k)}, \quad (3)$$

$$h_3^k = \frac{\mu_0}{4\pi} \gamma_S \gamma_{j_k} \frac{\mathbf{L}_k \cdot \mathbf{I}_k}{r_k^3(1 + d/r_k)}. \quad (4)$$

Here,  $\gamma_S = 2\mu_B$ ,  $\gamma_{j_k} = g_{j_k}\mu_N$ ,  $\mu_B$  is the Bohr magneton,  $g_{j_k}$  is the nuclear g-factor of isotopic species  $j_k$ ,  $\mu_N$  is the nuclear magneton,  $\mathbf{r}_k = \mathbf{r} - \mathbf{R}_k$  is the electron-spin position operator relative to the nucleus,  $d \simeq Z \times 1.5 \times 10^{-15}$  m is a length of nuclear dimensions,  $Z$  is the charge of the nucleus, and  $\mathbf{n}_k = \mathbf{r}_k/r_k$ .  $\mathbf{S}$  and  $\mathbf{L}_k = \mathbf{r}_k \times \mathbf{p}$  denote the spin and orbital angular-momentum operators of the electron, respectively. In Eq. (2) we have taken  $d \rightarrow 0$ , but have kept  $d$  finite in Eqs. (3) and (4) to avoid unphysical divergences when forming effective Hamiltonians [18].

Nuclear-spin interactions are typically much weaker than the spin-orbit interaction (see supplementary material). It is therefore appropriate to form effective Hamiltonians with respect to a basis of eigenstates of the Coulomb and spin-orbit interactions. The  $8 \times 8$  Kane Hamiltonian, which describes the band structure of a III-V semiconductor, provides such a basis [10, 11]. The Kane Hamiltonian is usually written in terms of conduction-band (CB) and valence-band (consisting of HH, light-hole (LH), and split-off sub-band) states. We derive an approximate basis of eigenstates in the HH sub-band by projecting the  $8 \times 8$  Kane Hamiltonian onto the two-dimensional HH subspace (see supplementary mate-

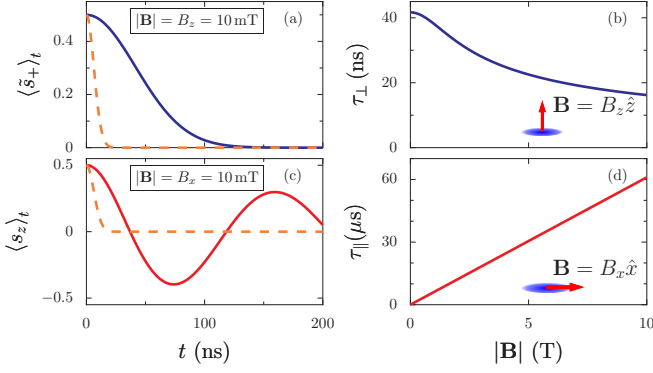


FIG. 1: Dephasing of HH pseudospin states (solid lines in (a) and (c)). The decay is Gaussian for an out-of-plane magnetic field  $B_z$  (a) (see Eq. (11)) and given by a slow power law at long times ( $\sim 1/\sqrt{t}$ ) for an in-plane magnetic field  $B_x$  (c) (see Eq. (12)). We have chosen  $|B| = 10$  mT in (a) and (c). Magnetic-field dependences of the relevant coherence times are shown for a field that is out-of-plane (b) and in-plane (d). We have assumed  $g_{\parallel} = 0.04$  [13] and a zero-field lateral dot size  $l_0 = 30$  nm and height  $a_z = 5$  nm, leading to  $N = \pi l_0^2 a_z / v_0 = 6.5 \times 10^5$  nuclei within the dot at  $B_z = 0$ . We have taken  $v_0 = a_L^3/8$ , where  $a_L = 5.65$  Å is the GaAs lattice constant. The dashed lines in (a) and (c) show the dephasing of CB electron spin states in the high-field limit,  $|B| \gg \sigma_e / g_e \mu_B$ , where  $g_e$  is the electron g-factor, and  $\sigma_e$  is obtained from Eq. (10) by replacing  $A_h^j$  by the electron hyperfine coupling constants  $A_e^j$ .

rial).

To form effective Hamiltonians, we must approximate the crystal-Hamiltonian eigenfunctions given by Bloch's theorem for a single band  $n$ :  $\Psi_{n\mathbf{k}\sigma}(\mathbf{r}) = \frac{1}{\sqrt{N_A}} e^{i\mathbf{k}\cdot\mathbf{r}} u_{n\mathbf{k}\sigma}(\mathbf{r})$ , where  $N_A$  is the number of atomic sites in the crystal, and the Bloch amplitudes  $u_{n\mathbf{k}\sigma}(\mathbf{r})$  have the periodicity of the lattice.

We will approximate the  $\mathbf{k} = \mathbf{0}$  Bloch amplitudes  $u_{n\mathbf{0}\sigma}(\mathbf{r})$  within a primitive unit cell by a linear combination of atomic orbitals (see Eq. (8), below). Near an atomic site, the CB Bloch amplitudes have approximate  $s$ -symmetry (angular momentum  $l = 0$ ), whereas the HH and LH Bloch amplitudes have approximate  $p$ -symmetry ( $l = 1$ ). Adding spin, the  $z$ -component of total angular momentum of a HH is  $m_J = \pm 3/2$ , whereas a LH has  $m_J = \pm 1/2$ . In the Q2D limit, i.e., going from the bulk crystal to a quantum well (whose growth direction we take to be [001]), a splitting  $\Delta_{\text{LH}}$  develops between the HH and LH sub-bands at  $\mathbf{k} = \mathbf{0}$ . We estimate  $\Delta_{\text{LH}} \simeq 100$  meV for a quantum well of height  $a_z \simeq 5$  nm in GaAs (see supplementary material), much larger than the hyperfine coupling (e.g.,  $A_e \simeq 90$   $\mu\text{eV}$  in the CB of GaAs [12]). The splitting  $\Delta_{\text{LH}}$  is essential since it produces a well-defined two-level system in the HH sub-band, and we can restrict our considerations to the manifold of  $m_J = \pm 3/2$  states.

Before addressing confinement in quantum dots, we

illustrate that the interaction of an electron in a hydrogenic  $p$  orbital with the spin of the nucleus (which we choose to be at  $\mathbf{R}_k = \mathbf{0}$ ) is generally non-zero. Moreover, when projected onto the manifold of  $m_J = \pm 3/2$  states, this interaction takes-on a simple Ising form. Although our final analysis will apply to any III-V semiconductor, we will take GaAs as a concrete example and for numerical estimates.

The effective screened nuclear charges  $Z_{\text{eff}}$  “felt” by the valence electrons (in  $4s$  and  $4p$  orbitals) in Ga and As atoms have been calculated in Ref. [14]. The  $4s$  orbitals and  $4p$  orbitals (with orbital angular momentum  $m_L = \pm 1$ ) are given in terms of hydrogenic eigenfunctions with the replacements  $Z \rightarrow Z_{\text{eff}}$  by  $\Psi_{400}(\mathbf{r}) = R_{40}(r)Y_0^0(\theta, \varphi)$  and  $\Psi_{41\pm 1}(\mathbf{r}) = R_{41}(r)Y_1^{\pm 1}(\theta, \varphi)$ , respectively. Including spin and evaluating matrix elements of the Hamiltonians (2)-(4) with respect to hydrogenic  $4s$  states leads to effective spin Hamiltonians of the form [9, 15]  $h_1^{4s} = A_s \mathbf{S} \cdot \mathbf{I}_k$  and, due to the spherical symmetry of the wavefunction,  $h_2^{4s} = h_3^{4s} = 0$ . The same procedure with the  $4p$  states leads to effective Hamiltonians  $h_1^{4p} = 0$  (since  $p$ -states vanish at the origin) and  $h_2^{4p} + h_3^{4p} = A_p s_z I_k^z$ , where  $s_z = \pm \frac{1}{2}$  corresponds to  $m_J = \pm 3/2$ .  $A_s$  and  $A_p$  denote the coupling strengths of electrons in  $4s$  and  $4p$  orbitals, respectively. Evaluating all integrals exactly gives

$$\frac{A_p}{A_s} = \frac{1}{5} \left( \frac{Z_{\text{eff}}(\kappa, 4p)}{Z_{\text{eff}}(\kappa, 4s)} \right)^3, \quad \kappa = \text{Ga, As.} \quad (5)$$

Quite significantly, after inserting values of  $Z_{\text{eff}}$  from Ref. [14] into Eq. (5), we find the ratio of coupling strengths is fairly large – on the order of 10%:  $A_p/A_s \simeq 0.14$  for Ga, and  $A_p/A_s \simeq 0.11$  for As. Since  $h_2^k$  and  $h_3^k$  do not contribute to the hyperfine interaction of an electron in an  $s$  orbital, research on hyperfine interaction for electrons in an  $s$ -type conduction band has focused on the contact term  $h_1^k$ , neglecting the other interactions. The fact that  $h_1^k$ , in contrast, gives no contribution for an electron in a  $p$  orbital has led to the claim that electrons in  $p$  orbitals (and holes) do not interact with nuclear spins. Eq. (5) shows that  $h_2^k$  and  $h_3^k$  can contribute significantly. Furthermore, while the interaction of a  $4s$ -electron with the nuclear spin is of Heisenberg type, within the manifold of  $m_J = \pm 3/2$  states, the interaction of a  $4p$ -electron is Ising-like at leading order (virtual transitions via the  $m_J = \pm 1/2$  states may lead to non-Ising corrections). This result is a direct consequence of the Wigner-Eckart theorem and the fact that the Hamiltonians (2)-(4) can be written in the form  $h_i^k = \mathbf{v}_i^k \cdot \mathbf{I}_k$ , where  $\mathbf{v}_i^k$  are vector operators in the electron (spin and orbital) Hilbert space.

We now return to the problem directly relevant to a HH in a two-dimensional quantum well. We consider an additional circular-symmetric parabolic confining potential in the plane of the quantum well defining a quantum dot. Neglecting hybridization with other bands, which we estimate to be typically on the order of 1% (see supplementary material), the pseudospin

states for a HH within the envelope-function approximation read  $|\Psi_\sigma\rangle = |\phi; u_{\text{HH}\mathbf{0}\sigma}\rangle|\sigma\rangle$ , where  $|\phi; u_{\text{HH}\mathbf{0}\sigma}\rangle$  and  $|\sigma\rangle$  ( $\sigma = \pm$ ) denote the orbital and spin states, respectively. The orbital wavefunctions are given explicitly by  $\langle \mathbf{r}|\phi; u_{\text{HH}\mathbf{0}\sigma}\rangle = \sqrt{v_0}\phi(\mathbf{r})u_{\text{HH}\mathbf{0}\sigma}(\mathbf{r})$ . Here,  $v_0$  is the volume occupied by a single atom (half the volume of a two-atom zinc-blende primitive unit cell), and  $\phi(\mathbf{r}) = \phi_z(z)\phi_\rho(\rho)$  is the envelope function (see supplementary material). The radial ground-state envelope function is a Gaussian:

$$\phi_\rho(\rho) = \frac{1}{\sqrt{\pi}l} \exp\left(-\frac{\rho^2}{2l^2}\right), \quad (6)$$

where  $\boldsymbol{\rho} = (x, y)$ ,  $\rho = |\boldsymbol{\rho}|$ ,  $l = l_0 [1 + (B_z/B_0)^2]^{-1/4}$ ,  $B_z$  is the component of an externally applied magnetic field along the growth direction and  $B_0 = \Phi_0/\pi l_0^2$  where  $\Phi_0 = h/e$  is a flux quantum. A typical dot Bohr radius of  $l_0 = 30$  nm gives  $B_0 \simeq 1.5$  T.

In a solid, the HH is delocalized over the lattice sites of the crystal. The nuclei do not interact solely with the fraction of the HH in the same primitive unit cell ('on-site' interaction), but also with density localized at more distant atomic sites (long-ranged interactions). We neglect the long-ranged interactions, which lead to corrections on the order of 1% relative to the on-site interaction (see supplementary material). If the envelope function varies slowly on the length scale of a primitive cell, we find (combining  $h_2^k$  and  $h_3^k$ )  $A_k^h = A_h^{jk} v_0 |\phi(\mathbf{R}_k)|^2$ , where

$$A_h^{jk} = -\frac{\mu_0}{4\pi} \gamma_S \gamma_{jk} \left\langle \frac{3 \cos^2 \theta_k + 1}{r_k^3 (1 + d/r_k)} \right\rangle_{\text{p.c.}}. \quad (7)$$

Here,  $\langle \dots \rangle_{\text{p.c.}}$  denotes the expectation value with respect to  $u_{\text{HH}\mathbf{0}\sigma}(\mathbf{r})$  over a primitive unit cell ( $\sigma = \pm$  give the same matrix elements), and  $\theta_k$  is the polar angle of  $\mathbf{r}_k$ . The magnetic moment of a HH is inverted with respect to that for an electron. This results in a change of sign in Eqs. (2)-(4) and leads to the minus sign in Eq. (7) and of the values in columns (i) and (ii) of Table I.

To estimate the size of  $A_h^j$ , we need an explicit expression for the HH  $\mathbf{k} = \mathbf{0}$  Bloch amplitudes. We approximate  $u_{\text{HH}\mathbf{0}\sigma}(\mathbf{r})$  within a Wigner-Seitz cell centered halfway along the Ga-As bond by a linear combination of atomic orbitals, following Ref. [16]:

$$u_{\text{HH}\mathbf{0}\sigma}(\mathbf{r}) \Big|_{\mathbf{r} \in \text{WS}} = N_{\alpha_v} \left( \alpha_v \Psi_{41\sigma}^{\text{Ga}}(\mathbf{r} + \mathbf{d}/2) + \sqrt{1 - \alpha_v^2} \Psi_{41\sigma}^{\text{As}}(\mathbf{r} - \mathbf{d}/2) \right). \quad (8)$$

$u_{\text{HH}\mathbf{0}\sigma}$  is then defined over the entire crystal via the condition:  $u_{\text{HH}\mathbf{0}\sigma}(\mathbf{r}) = u_{\text{HH}\mathbf{0}\sigma}(\mathbf{r} + \mathbf{R})$ , where  $\mathbf{R}$  is any lattice translation. Here,  $\mathbf{d} = \frac{a}{4}(1, 1, 1)$  is the Ga-As bond vector,  $a$  is the lattice constant,  $\alpha_v$  describes the relative electron sharing at the Ga and As sites in the HH sub-band, and  $N_{\alpha_v}$  is a normalization constant, chosen to enforce  $\int_{\text{WS}} d^3r |u_{\text{HH}\mathbf{0}\sigma}(\mathbf{r})|^2 = 2$ , where the integration is performed over the Wigner-Seitz cell defined

j	$A_h^j$ ( $\mu\text{eV}$ )		$A_e^j$ ( $\mu\text{eV}$ )	
	(i)	(ii)	(iii)	(iv)
$^{69}\text{Ga}$	-7.1	-13	40	74
$^{71}\text{Ga}$	-9.0	-17	51	94
$^{75}\text{As}$	-8.2	-12	59	89
$A_\alpha = \sum_j \nu_j A_\alpha^j$ ( $\alpha = e, h$ )	-8.0	-13	52	86

TABLE I: Estimates of the coupling strengths for a HH ( $A_h^j$ ) and a CB electron ( $A_e^j$ ) for the three isotopes in GaAs. Columns (i) and (iii) show values obtained from a linear combination of hydrogenic eigenfunctions, using free-atom values of  $Z_{\text{eff}}$  calculated in Ref. [14]. Column (iv) gives the accepted values of  $A_e^j$  from Ref. [12]. Column (ii) shows the rescaled values from column (i) (see text). In the last row we give the average coupling constants weighted by the natural isotopic abundances:  $\nu_{^{69}\text{Ga}} = 0.3$ ,  $\nu_{^{71}\text{Ga}} = 0.2$ ,  $\nu_{^{75}\text{As}} = 0.5$ .

above. To simplify numerical integration, we replace the Wigner-Seitz cell by a sphere centered halfway along the Ga-As bond, with radius given by half the Ga-Ga nearest-neighbor distance. We find the electron sharing in the CB from the densities given in Ref. [12] to be  $\alpha_c^2 \simeq 1/2$  (see supplementary material) and assume the same ( $\alpha_v^2 = 1/2$ ) for Eq. (8). Using  $Z_{\text{eff}}$  for free atoms [14], we evaluate Eq. (7) with the ansatz, Eq. (8), by numerical integration, giving the values shown in Table I, column (i). We check the validity of this procedure by writing the CB Bloch amplitudes as in Eq. (8), replacing the  $4p$ -eigenfunctions by  $4s$ -eigenfunctions (see supplementary material). Evaluating the coupling constants for the CB ( $A_e^j$ ) from  $h_1^k$  gives the numbers in column (iii). The accepted values of  $A_e^j$  from Ref. [12] are shown in column (iv) for comparison. Our method produces  $A_e^j$  to within a factor of two of the accepted values. Based on the results in columns (iii) and (iv), we conclude that our procedure most likely under-estimates the electron density near the atomic sites. Assuming that the relative deviation is the same for the CB and the HH band, we rescale the results in column (i) by the ratio of the values in columns (iv) and (iii), giving column (ii). Due to the approximations involved, we expect the values columns (i) and (ii) only to be valid to within a factor of two or three.

There will be corrections to the form of the effective Hamiltonian given in Eq. (1). Small non-Ising terms could arise from several sources. Evaluating off-diagonal matrix elements of (3) and (4) with the approximate Bloch amplitudes (8) yields non-Ising terms, whose associated coupling strengths  $A_h^\perp$  we find to be small:  $A_h^\perp < 0.06 A_h^j$ . Higher-order virtual transitions between the  $m_J = \pm 3/2$  states via the LH sub-band are suppressed by  $\sim A_k^h/\Delta_{\text{LH}} \ll 1$ . Hybridization with other bands can also lead to non-Ising corrections, which we find to be small (typically on the order of 1% of the values given in Table I, see supplementary material).

Now that the effective Hamiltonian (Eq. (1)) has been

established, we can analyze the dephasing of a HH pseudospin in the presence of a random nuclear environment. In an applied magnetic field, pseudospin dynamics of the HH are described by the Hamiltonian

$$H = (b_{\perp} + h_z) s_z + b_{\parallel} s_x, \quad (9)$$

where  $h_z = \sum_k A_k^h I_k^z$  is the nuclear field operator,  $b_{\perp} = g_{\perp} \mu_B B_z$  is the Zeeman splitting due to a magnetic field  $B_z$  along the growth direction, and  $b_{\parallel} = g_{\parallel} \mu_B B_x$  is the Zeeman splitting due to an applied magnetic field  $B_x$  in the plane of the quantum dot.  $g_{\perp}$  and  $g_{\parallel}$  are the components of the HH  $g$ -tensor along the growth direction and in the plane of the quantum dot, respectively (we assume the in-plane  $g$ -tensor to be isotropic).

If no special effort is made to control the nuclear field, the field value will be Gaussian-distributed in the limit of a large number of nuclear spins [5]. The variance for a random (infinite-temperature) nuclear-spin distribution is (see supplementary material)

$$\langle h_z^2 \rangle = \sigma^2 \simeq \frac{1}{4N} \sum_j \nu_j I^j (I^j + 1) (A_h^j)^2, \quad (10)$$

where  $N = \pi l^2 a_z / v_0$  is the number of nuclei within the quantum dot. The nuclear-field fluctuation  $\sigma$  therefore inherits a magnetic-field dependence from  $l$  (see Eq. (6)). A finite nuclear-field variance will result in a random distribution of precession frequencies experienced by the hole pseudospin, inducing pure dephasing (decay of the components of hole pseudospin transverse to  $\mathbf{B}$ ).

First, we consider the case  $b_{\parallel} = 0$ . For a hole pseudospin initially oriented along the  $x$  direction, we find a Gaussian decay (see Fig. 1 (a)) of the transverse pseudospin in the rotating frame  $\langle \tilde{s}_+ \rangle_t = \exp(-ib_{\perp} t) (\langle s_x \rangle_t + i \langle s_y \rangle_t)$ :

$$\langle \tilde{s}_+ \rangle_t = \frac{1}{2} \exp\left(-\frac{t^2}{2\tau_{\perp}^2}\right), \quad \tau_{\perp} = \frac{1}{\sigma}. \quad (11)$$

This is the same Gaussian decay that occurs for electrons [4, 5]. Here, since the magnetic field is taken to be out-of-plane, we must take account of the diamagnetic “squeezing” of the wavefunction. This squeezing affects the number  $N$  of nuclear spins within the dot and hence, the finite-size fluctuation  $\sigma$ . The coherence time  $\tau_{\perp}(B_z) = 1/\sigma(B_z) = \tau_{\perp}(0) [1 + (B_z/B_0)^2]^{-1/4}$  then *decreases* for large  $B_z$  (see Fig. 1 (b)). This undesirable effect can be avoided for confined electron spins by generating a large Zeeman splitting through an in-plane (rather than out-of-plane) magnetic field. This option may not be available for a HH where, typically,  $g_{\parallel} \ll g_{\perp}$ .

The situation changes drastically for an in-plane magnetic field ( $b_{\perp} = 0$ ). In this case, the decay is given by a slow power law at long times (see Fig. 1 (c)) and the relevant dephasing time *increases* as a function of the applied magnetic field (see Fig. 1 (d)). In the limit

$b_{\parallel} \gg \sigma$  and for a HH pseudospin initially prepared along the  $\hat{z}$ -direction, we find

$$\langle s_z \rangle_t \simeq \frac{\cos(b_{\parallel} t + \frac{1}{2} \arctan(t/\tau_{\parallel}))}{2[1 + (\frac{t}{\tau_{\parallel}})^2]^{1/4}}, \quad \tau_{\parallel} = \frac{b_{\parallel}}{\sigma^2}. \quad (12)$$

The derivation of Eq. (12) is directly analogous to that for the decay of driven Rabi oscillations in Ref. [17].

The interaction with nuclear spins can be the main source of decoherence for a quantum-dot-confined HH. However, the form of the interaction may allow for an effective extension of the coherence time by controlling the nuclear environment. The strong coupling of the HH to the nuclear spins is not a consequence of confinement but is also present in bulk crystals. The Ising-like interaction we find is a feature of Q2D systems, in particular also of quantum wells.

We acknowledge discussions with S. I. Erlingsson and D. Stepanenko, and funding from the Swiss NSF, NCCR Nanoscience, JST ICORP, QuantumWorks, an Ontario PDF (WAC), and the “Dynasty” Foundation (DVB).

- 
- [1] D. Loss and D. P. DiVincenzo, Phys. Rev. A **57**, 120 (1998).
  - [2] V. Cerletti *et al.*, Nanotechnology **16**, R27 (2005).
  - [3] G. Burkard, D. Loss, and D. P. DiVincenzo, Phys. Rev. B **59**, 2070 (1999).
  - [4] I. A. Merkulov, A. L. Efros, and M. Rosen, Phys. Rev. B **65**, 205309 (2002); A. V. Khaetskii, D. Loss, and L. Glazman, Phys. Rev. Lett. **88**, 186802 (2002).
  - [5] W. A. Coish and D. Loss, Phys. Rev. B **70**, 195340 (2004).
  - [6] J. R. Petta *et al.*, Science **309**, 2180 (2005).
  - [7] D. Heiss *et al.*, Phys. Rev. B **76**, 241306 (2007); B. D. Gerardot *et al.*, Nature **451**, 441 (2008); A. J. Ramsay *et al.*, Phys. Rev. Lett. **100**, 197401 (2008).
  - [8] T. Flissikowski *et al.*, Phys. Rev. B **68**, 161309 (2003); A. Shabaev *et al.*, *ibid.* **68**, 201305 (2003); L. M. Woods, T. L. Reinecke, and R. Kotlyar, *ibid.* **69**, 125330 (2004); D. V. Bulaev and D. Loss, Phys. Rev. Lett. **95**, 076805 (2005); S. Laurent *et al.*, *ibid.* **94**, 147401 (2005); D. V. Bulaev and D. Loss, *ibid.* **98**, 097202 (2007); Y. A. Serebrennikov, arXiv:0710.1446; G. Burkard, Nature Materials **7**, 100 (2008).
  - [9] A. M. Stoneham, *Theory of Defects in Solids* (Oxford University Press, 1972), chapter 13.
  - [10] R. Winkler, *Spin-Orbit Coupling Effects in Two-Dimensional Electron and Hole Systems* (Springer, 2003), chapter 3.
  - [11] P. Y. Yu and M. Cardona, *Fundamentals of Semiconductors* (Springer, 2005), section 2.6.
  - [12] D. Paget *et al.*, Phys. Rev. B **15**, 5780 (1977).
  - [13] X. Marie *et al.*, Phys. Rev. B **60**, 5811 (1999).
  - [14] E. Clementi and D. L. Raimondi, J. Chem. Phys. **38**, 2686 (1963).
  - [15] A. Abragam, *The Principles of Nuclear Magnetism* (Oxford University Press, 1961), section VI.II.
  - [16] M. Gueron, Phys. Rev. **135**, A200 (1964).

- [17] F. H. L. Koppens *et al.*, Phys. Rev. Lett. **99**, 106803 (2007), see especially the associated auxiliary material (EPAPS Document No. E-PRLTAO-99-027736).
- [18] In Ref. [15], these divergences are avoided by expanding the wavefunction in terms of spherical harmonics. Keeping  $d$  finite, as in Ref. [9], leads to equivalent results.

**SUPPLEMENTARY MATERIAL FOR “SPIN DECOHERENCE OF A HEAVY HOLE COUPLED TO NUCLEAR SPINS IN A QUANTUM DOT”**

**Heavy-hole states**

In this section we give details on our derivation of an approximate basis of heavy-hole (HH) eigenstates in a quantum dot. We will approximate the ground-state quantum-dot envelope function in the HH sub-band by

$$\phi(\mathbf{r}) = \phi_z(z) \phi_\rho(\rho), \quad (\text{S1})$$

$$\phi_\rho(\rho) = \frac{1}{\sqrt{\pi}l} \exp\left(-\frac{\rho^2}{2l^2}\right), \quad (\text{S2})$$

$$\phi_z(z) = \sqrt{\frac{2}{a_z}} \sin\left(\frac{\pi z}{a_z}\right), \quad z = [0 \dots a_z], \quad (\text{S3})$$

where  $a_z$  is the width of the confinement potential along the growth direction (for definition of the other symbols see Eq. (6) of the main text). We will then estimate the size of the splitting  $\Delta_{\text{LH}}$  between the HH and the light-hole (LH) band and the degree of hybridization with the conduction band (CB), LH and split-off (SO) sub-bands.

We start from the  $8 \times 8$  Kane Hamiltonian given in Ref. [S1] for bulk zinc-blende-type crystals, which is written in terms of the exact eigenstates (near  $\mathbf{k} = \mathbf{0}$ ) of an electron in the CB, HH, LH and SO band, usually denoted by  $|1/2; \pm 1/2\rangle_c$ ,  $|3/2; \pm 3/2\rangle_v$ ,  $|3/2; \pm 1/2\rangle_v$ , and  $|1/2; \pm 1/2\rangle_v$ , respectively. We neglect terms that are more than two orders of magnitude smaller than the fundamental band-gap energy  $E_g$  [S7] and perform the quasi-two-dimensional limit by assuming that a confinement potential has been applied along the growth direction. If the confinement potential is sufficiently strong (i.e., if the quantum well is sufficiently narrow), the energy-level spacing will be large and the electron will be in the ground state at low temperatures. Any operator acting on the  $z$ -component of the electron envelope function can then be replaced by its expectation value with respect to the  $z$ -component of the ground-state envelope function. For the Kane Hamiltonian this means that we can replace powers of the  $z$ -component  $\hbar k_z$  of the crystal momentum  $\hbar \mathbf{k}$  by expectation values. Assuming an infinite square-well potential of width  $a_z$  confining the electron along the growth direction, the ground state is given by Eq. (S3). Calculating the expectation value of  $k_z$  and  $k_z^2$  with respect to the ground state, we find  $\langle k_z \rangle = 0$  and  $\langle k_z^2 \rangle = \pi^2/a_z^2$ . This allows us to write the Kane Hamiltonian in the following form:

$$H_K = \begin{pmatrix} H_{\text{CB}} & V_1 & V_2 & V_3 \\ V_1^\dagger & H_{\text{HH}} & V_4 & V_5 \\ V_2^\dagger & V_4^\dagger & H_{\text{LH}} & V_6 \\ V_3^\dagger & V_5^\dagger & V_6^\dagger & H_{\text{SO}} \end{pmatrix}, \quad (\text{S4})$$

where

$$\begin{aligned} H_{\text{CB}} &= \begin{pmatrix} A & 0 \\ 0 & A \end{pmatrix}, & H_{\text{HH}} &= \begin{pmatrix} B & 0 \\ 0 & B \end{pmatrix}, \\ H_{\text{LH}} &= \begin{pmatrix} C & 0 \\ 0 & C \end{pmatrix}, & H_{\text{SO}} &= \begin{pmatrix} D & 0 \\ 0 & D \end{pmatrix}, \\ V_1 &= \frac{1}{\sqrt{2}} \begin{pmatrix} -E & 0 \\ 0 & E^* \end{pmatrix}, & V_2 &= \frac{1}{\sqrt{6}} \begin{pmatrix} 0 & E^* \\ -E & 0 \end{pmatrix}, \\ V_3 &= \frac{1}{\sqrt{3}} \begin{pmatrix} 0 & -E^* \\ -E & 0 \end{pmatrix}, & V_4 &= \sqrt{3} \begin{pmatrix} 0 & F \\ F^* & 0 \end{pmatrix}, \\ V_5 &= \sqrt{6} \begin{pmatrix} 0 & -F \\ F^* & 0 \end{pmatrix}, & V_6 &= \sqrt{2} \begin{pmatrix} -G & 0 \\ 0 & G \end{pmatrix}, \end{aligned}$$

and

$$\begin{aligned} A &= E_g + \hbar^2(k_x^2 + k_y^2 + \langle k_z^2 \rangle)/2m', \\ B &= -\epsilon[(\gamma'_1 + \gamma'_2)(k_x^2 + k_y^2) + (\gamma'_1 - 2\gamma'_2)\langle k_z^2 \rangle], \\ C &= -\epsilon[(\gamma'_1 - \gamma'_2)(k_x^2 + k_y^2) + (\gamma'_1 + 2\gamma'_2)\langle k_z^2 \rangle], \\ D &= -\epsilon\gamma'_1(k_x^2 + k_y^2 + \langle k_z^2 \rangle) - \Delta_{\text{SO}}, \\ E &= Pk_+, \\ F &= \epsilon[\gamma'_2(k_x^2 - k_y^2) - 2i\gamma'_3 k_x k_y], \\ G &= \epsilon\gamma'_2(k_x^2 + k_y^2 - 2\langle k_z^2 \rangle). \end{aligned}$$

Here,  $\epsilon = \hbar^2/2m_0$  and  $m_0$  is the free-electron mass, whereas  $m'$  is the effective mass of a CB electron. Furthermore,  $k_\pm = k_x \pm ik_y$ ,  $\gamma'_j$  denote the Luttinger parameters,  $P$  is the inter-band momentum, and  $\Delta_{\text{SO}}$  is the spin-orbit gap between the LH and the SO bands. Experimental values for these parameters can be found in Table II.

We assume a circular-symmetric parabolic confinement potential with frequency  $\omega_0$  in the  $xy$ -plane defining a quantum dot. Including a magnetic field along the growth direction, the ground state is approximately described by the Gaussian given in Eq. (S2). The envelope function of the quantum dot is then the product of the in-plane and out-of-plane components, as given in Eq. (S1).

In the quasi-two-dimensional limit, a gap

$$\Delta_{\text{LH}} = \langle B - C \rangle = -\frac{\hbar^2 \gamma'_2}{m_0} (\langle k_x^2 \rangle + \langle k_y^2 \rangle - 2\langle k_z^2 \rangle) \quad (\text{S5})$$

develops between the HH and LH sub-bands, lifting the HH-LH degeneracy. Here,  $\langle \dots \rangle$  denotes the expectation value with respect to (S1). The in-plane level spacing scales like  $\sim 1/l^2$ , where  $l$  is the dot Bohr radius. The in-plane level spacing is much smaller than the level spacing along the growth direction since, for typical dots,  $a_z^2 \ll l^2$ . Neglecting  $\langle k_x^2 \rangle$  and  $\langle k_y^2 \rangle$  compared to  $\langle k_z^2 \rangle$  in Eq. (S5) and inserting  $\langle k_z^2 \rangle = \pi^2/a_z^2$  for a square-well potential, we estimate

$$\Delta_{\text{LH}} \simeq \frac{2\pi^2 \gamma'_2 \hbar^2}{a_z^2 m_0} \simeq 100 \text{ meV} \quad (\text{S6})$$

for  $a_z \simeq 5$  nm, using  $\gamma'_2 \simeq 2.06$  for GaAs (see Table II). The HH-LH splitting is thus much larger than the typical energy scale associated with the hyperfine interaction ( $A_e \simeq 90 \mu\text{eV}$  for CB electrons in GaAs).

To derive the approximate electron eigenfunctions in the HH sub-band of the quantum well, we start from the Kane Hamiltonian (S4). We use quasi-degenerate perturbation theory up to first order in  $1/\mathcal{E}$  (where  $\mathcal{E}$  stands for  $E_g$ ,  $\Delta_{\text{LH}}$ , or  $\Delta_{\text{LH}} + \Delta_{\text{SO}}$ ), taking  $H_{\text{HH}}$  as the unperturbed Hamiltonian [S1]. This leads to a band-hybridized state of the form

$$|\Psi_{\text{HH,hyb}}^\sigma\rangle = \mathcal{N}_\sigma \sum_n \lambda_n^\sigma |\phi_{n\sigma}; u_{n\mathbf{0}\sigma}\rangle. \quad (\text{S7})$$

Here,  $\sigma = \pm$ ,  $\langle \mathbf{r} | \phi_{n\sigma}; u_{n\mathbf{0}\sigma} \rangle = \sqrt{v_0} \phi_{n\sigma}(\mathbf{r}) u_{n\mathbf{0}\sigma}(\mathbf{r})$  is the product of envelope function and  $\mathbf{k} = \mathbf{0}$  Bloch amplitude in band  $n$  (CB, HH, LH or SO), the prefactors  $\lambda_n^\sigma$  describe the degree of band hybridization, and  $\mathcal{N}_\sigma$  enforces proper normalization.

In first order quasi-degenerate perturbation theory, the hybridization with the CB and the LH and SO sub-bands is described by the interaction terms  $V_1$ ,  $V_4$ , and  $V_5$  in Eq. (S4), respectively. We estimate the degree of hybridization by applying these operators to a two-spinor containing the in-plane ground-state envelope function (S2) of the HH sub-band. For the hybridization with the conduction band, we find (for  $\mathbf{B} = \mathbf{0}$ )

$$-\frac{1}{E_g} V_1 \begin{pmatrix} \phi_\rho(\rho) \\ \phi_\rho(\rho) \end{pmatrix} = \begin{pmatrix} \lambda_{\text{CB}}^+ \phi_{\text{CB}\rho+}(\rho) \\ \lambda_{\text{CB}}^- \phi_{\text{CB}\rho-}(\rho) \end{pmatrix}, \quad (\text{S8})$$

where

$$\phi_{\text{CB}\rho\pm}(\rho) = \frac{i}{\sqrt{2}} (\psi_{10}(\rho) \pm i\psi_{01}(\rho)). \quad (\text{S9})$$

Here,  $\psi_{nm}(\rho) = \psi_n(x)\psi_m(y)$  and  $\psi_n(x)$  is the  $n^{\text{th}}$  harmonic-oscillator eigenstate. The envelope function of the admixed CB state is a superposition of *excited* harmonic-oscillator eigenfunctions. The prefactor

$$\lambda_{\text{CB}}^\pm = \pm \frac{P}{\sqrt{2}E_g l_0} \quad (\text{S10})$$

determines the degree of  $sp$ -hybridization. Using values from Table II and assuming a quantum dot with dot Bohr radius  $l_0 \simeq 30$  nm ( $\mathbf{B} = \mathbf{0}$ ), we estimate  $\lambda_{\text{CB}}^\pm \simeq 10^{-2}$ . Similarly, we estimate  $\lambda_{\text{LH}}^\pm \simeq \lambda_{\text{SO}}^\pm \simeq 10^{-3}$ , assuming a dot height  $a_z \simeq 5$  nm. The admixture of CB, LH and SO states to the HH state is thus on the order of 1% and has therefore been neglected in our considerations in the main text.

We emphasize that  $sp$ -hybridization will lead to a coupling of the HH to the nuclear spins via the Fermi contact interaction (Eq. (2) in the main text). Since the Fermi contact interaction is of Heisenberg-type,  $sp$ -hybridization will directly lead to non-Ising corrections

$P$ (eVÅ)	10.5*	$\gamma'_1$	6.98†
$E_g$ (eV)	1.52*	$\gamma'_2$	2.06†
$\Delta_{\text{SO}}$ (eV)	0.34*	$\gamma'_3$	2.93†

TABLE II: Values of band parameters used in this section; \*taken from Ref. [S1]; †taken from Ref. [S2].

to the effective Hamiltonian given in Eq. (1) in the main text. The size of these corrections is determined by the degree of  $sp$ -hybridization which is on the order of 1% (see above).

### Estimate of the Fermi contact interaction

In Eq. (8) of the main text, we have approximated the HH  $\mathbf{k} = \mathbf{0}$  Bloch amplitudes within a Wigner-Seitz cell by a linear combination of atomic orbitals. Similarly, we approximate the  $\mathbf{k} = \mathbf{0}$  Bloch amplitude in the CB by

$$u_{\text{CB}\mathbf{0}\sigma}(\mathbf{r}) \Big|_{\mathbf{r} \in \text{WS}} = N_{\alpha_c} \left( \alpha_c \Psi_{400}^{\text{Ga}}(\mathbf{r} + \mathbf{d}/2) - \sqrt{1 - \alpha_c^2} \Psi_{400}^{\text{As}}(\mathbf{r} - \mathbf{d}/2) \right), \quad (\text{S11})$$

independent of  $\sigma$ . Here,  $\Psi_{400}(\mathbf{r}) = R_{40}(r)Y_0^0(\theta, \varphi)$ ,  $\alpha_c$  describes the relative electron sharing between the Ga and As atom in the Wigner-Seitz cell chosen to be centered halfway along the Ga-As bond, and  $N_{\alpha_c}$  normalizes the Bloch amplitude to two atoms in a primitive unit cell. The radial wavefunction depends implicitly on the effective nuclear charges  $Z_{\text{eff}}(\kappa, 4s)$ , where  $\kappa = \text{Ga, As}$ .

We will estimate the relative electron sharing in the CB by calculating the electron densities at the sites of the nuclei from Eq. (S11) and comparing to accepted values taken from Ref. [S3]. We will then estimate the Fermi contact interaction of a CB electron using free-atom effective nuclear charges taken from Ref. [S4] ( $Z_{\text{eff}}(\text{Ga}, 4s) \simeq 7.1$ ,  $Z_{\text{eff}}(\text{Ga}, 4p) \simeq 6.2$ ,  $Z_{\text{eff}}(\text{As}, 4s) \simeq 8.9$ , and  $Z_{\text{eff}}(\text{As}, 4p) \simeq 7.4$ ) and normalizing the Bloch amplitude over a Wigner-Seitz cell.

We approximate the electron densities at the Ga and As sites within a primitive unit cell from Eq. (S11):

$$d_{\text{Ga}} = |u_{\text{CB}\mathbf{0}\sigma}(-\mathbf{d}/2)|^2 \simeq N_{\alpha_c}^2 \alpha_c^2 |\Psi_{400}^{\text{Ga}}(\mathbf{0})|^2, \quad (\text{S12})$$

$$d_{\text{As}} = |u_{\text{CB}\mathbf{0}\sigma}(+\mathbf{d}/2)|^2 \simeq N_{\alpha_c}^2 (1 - \alpha_c^2) |\Psi_{400}^{\text{As}}(\mathbf{0})|^2. \quad (\text{S13})$$

We estimate the corrections to the right-hand sides to be on the order of 1% due to overlap terms. We take the ratio  $d_{\text{Ga}}/d_{\text{As}}$  and equate this with the ratio of the values from Ref. [S3],  $d'_{\text{Ga}} = 5.8 \times 10^{-31} \text{ m}^{-3}$  and  $d'_{\text{As}} = 9.8 \times 10^{-31} \text{ m}^{-3}$ . This allows us to write  $\alpha_c$  as a function of the two effective nuclear charges:

$$\alpha_c = \left[ 1 + \frac{d'_{\text{As}}}{d'_{\text{Ga}}} \left( \frac{Z_{\text{eff}}(\text{Ga}, 4s)}{Z_{\text{eff}}(\text{As}, 4s)} \right)^3 \right]^{-1/2}. \quad (\text{S14})$$

Recalling that  $N_{\alpha_c}$  normalizes the Bloch amplitude to two atoms over a Wigner-Seitz cell, we write

$$N_{\alpha_c} = \left[ \frac{1}{2} \int_{\text{WS}} d^3r \left| \alpha_c \Psi_{400}^{\text{Ga}}(\mathbf{r} + \mathbf{d}/2) - \sqrt{1 - \alpha_c^2} \Psi_{400}^{\text{As}}(\mathbf{r} - \mathbf{d}/2) \right|^2 \right]^{-1/2}. \quad (\text{S15})$$

For all numerical integrations, we approximate the Wigner-Seitz cell by a sphere centered halfway along the Ga-As bond with radius equal to half the Ga-Ga nearest-neighbor distance. Inserting (S14) and (S15) into (S12) and (S13), we solve the two coupled equations

$$d_{\text{Ga}}(Z_{\text{eff}}(\text{Ga}), Z_{\text{eff}}(\text{As})) - d'_{\text{Ga}} = 0, \quad (\text{S16})$$

$$d_{\text{As}}(Z_{\text{eff}}(\text{Ga}), Z_{\text{eff}}(\text{As})) - d'_{\text{As}} = 0, \quad (\text{S17})$$

for the two effective nuclear charges. This yields  $Z_{\text{eff}}(\text{Ga}) \simeq 9.8$  and  $Z_{\text{eff}}(\text{As}) \simeq 11.0$ . Inserting these values back into Eq. (S14), we estimate the electron sharing within the primitive unit cell to be

$$\alpha_c^2 \simeq 0.46. \quad (\text{S18})$$

For comparison, inserting free-atom effective nuclear charges into Eq. (S14) yields a similar value:  $\alpha_c'^2 \simeq 0.54$ .

Now we estimate the Fermi contact interaction of a CB electron starting from the free-atom effective nuclear charges  $Z_{\text{eff}}(\kappa, 4s)$  obtained from Ref. [S4]. We use  $\alpha_c \simeq 1/\sqrt{2}$  and normalize the  $\mathbf{k} = \mathbf{0}$  Bloch amplitude to two atoms over a Wigner-Seitz cell, following Eq. (S15). From the normalized Bloch amplitudes we estimate the Fermi contact hyperfine interaction by evaluating

$$A_e^j = \frac{2\mu_0}{3} \gamma_S \gamma_j |u_{\text{CB}\mathbf{0}\sigma}(\mathbf{R}_j)|^2. \quad (\text{S19})$$

Here,  $\mathbf{R}_j = \mp \mathbf{d}/2$  for Ga and As, respectively ( $j$  indexes the nuclear isotope). Evaluating for the isotopes in GaAs, this gives the values shown in column (iii) of Table I in the main text.

Replacing the Wigner-Seitz cell by a sphere with radius  $R_s$  equal to half the Ga-Ga nearest-neighbor distance in our numerical integrations overestimates the expectation value of  $[r_k^3(1 + d/r_k)]^{-1}$  in Eq. (7) of the main text. To estimate the error, we perform an integration over a sphere with radius  $R'_s = (R_s + R_{\text{max}})/2$ , where  $R_{\text{max}}$  denotes the radius of the smallest sphere that fully contains the Wigner-Seitz cell. From this, we estimate the relative error to be less than 30%.

### Estimate of the long-ranged interactions

In this section, we estimate corrections to the HH coupling strength (Eq. (7) in the main text) due to long-ranged dipole-dipole interactions and long-ranged  $\mathbf{L} \cdot \mathbf{I}$

interactions. To this end, we consider a single nucleus interacting with a HH that is delocalized over the lattice sites in the quantum dot. We start from the Hamiltonians given in Eqs. (3) and (4) in the main text. We define effective radii  $a_{\text{eff}}(\kappa, 4p) = a_0/Z_{\text{eff}}(\kappa, 4p)$ , where  $a_0 \simeq 5.3 \times 10^{-11} \text{ m}$  is the Bohr radius. The effective radii define an approximate length scale for the spread of the site-localized functions  $\Psi_{41\sigma}^{\kappa}(\mathbf{r})$  and are much smaller than the GaAs lattice constant  $a_L \simeq 5.7 \times 10^{-10} \text{ m}$ . The nucleus thus effectively ‘sees’ sharp-peaked electron densities centered around the more distant lattice sites. We choose the nucleus to be at site  $\mathbf{R}_k$  and estimate the interaction with the electron density at more distant atomic sites by approximating the electron densities by  $\delta$ -functions. Adding up contributions from  $h_2^k$  and  $h_3^k$ , we arrive at an effective Hamiltonian describing the long-ranged interactions:  $H_{\text{lr}}^k = A_{\text{lr}}^k s_z I_k^z$ , where  $A_{\text{lr}}^k = \sum_{l;l \neq k} A_{\text{lr}}^{kl}$  is the associated coupling strength and  $A_{\text{lr}}^{kl} = v_0 |\phi(\mathbf{R}_l)|^2 \int d^3r_k \{\delta(\mathbf{r}_k - \mathbf{R}_{kl})(h_2^k + h_3^k)\}$  describes the coupling of the electron density at site  $\mathbf{R}_l$  to the nucleus at site  $\mathbf{R}_k$  ( $\mathbf{R}_{kl} = \mathbf{R}_l - \mathbf{R}_k$ ). In order to estimate the size of the long-ranged interactions relative to the on-site interactions, we take into account nearest-neighbor couplings for the long-ranged part, i.e., we replace  $\sum_{l;l \neq k} \rightarrow \sum_{l=\text{n.n.}}$ . The interaction with electron density located around more distant nuclei is suppressed by  $\sim 1/R_{kl}^3$ . Assuming that the quantum-dot envelope function varies slowly over the nearest-neighbor distance ( $\phi(\mathbf{R}_l) \simeq \phi(\mathbf{R}_k)$  for  $l$  nearest neighbor of  $k$ ), we estimate the ratio of long-ranged and on-site interactions (Table I, column (i) in the main text) to be

$$\frac{A_{\text{lr}}}{A_h} \simeq 7 \times 10^{-3}, \quad (\text{S20})$$

on the order of 1%, where  $A_{\text{lr}}^k = A_{\text{lr}} v_0 |\phi(\mathbf{R}_k)|^2$ .

We remark that, in principle, the electron g-factor can deviate from the free-electron g-factor due to spin-orbit interaction. According to Ref. [S5], this renormalization is negligible for the on-site interaction, but could become relevant for the long-ranged interaction. However, for the estimate in Eq. (S20), we have taken the free-electron g-factor.

### Variance of the nuclear field

Here we calculate the nuclear-field variance for a HH interacting with nuclei in a quantum dot. In particular, we evaluate

$$\sigma^2 = \langle h_z^2 \rangle, \quad (\text{S21})$$

where  $\langle \dots \rangle = \text{Tr}_I (\bar{\rho}_I \dots)$  indicates the expectation value with respect to the infinite-temperature thermal equilibrium density matrix  $\bar{\rho}_I$  and we recall  $h_z = \sum_k A_k^h I_k^z$ . For



an uncorrelated and unpolarized nuclear state, we have  $\langle I_k^z I_{k'}^z \rangle = \langle I_k^z \rangle \langle I_{k'}^z \rangle = 0$ ,  $k \neq k'$ , which gives

$$\sigma^2 = \sum_k (A_k^h)^2 \langle (I_k^z)^2 \rangle. \quad (\text{S22})$$

Using  $\langle (I_k^z)^2 \rangle = I^{j_k} (I^{j_k} + 1) / 3$  for an infinite-temperature state,  $A_k^h = A_h^{j_k} v_0 |\phi(\mathbf{R}_k)|^2$ , and assuming that the nuclear isotopic species with abundances  $\nu_j$  are distributed uniformly throughout the dot gives

$$\sigma^2 = \frac{1}{3} I_0 \sum_j \nu_j I^j (I^j + 1) (A_h^j)^2, \quad (\text{S23})$$

where

$$I_0 = v_0^2 \sum_k |\phi(\mathbf{R}_k)|^4. \quad (\text{S24})$$

Assuming that the envelope function  $\phi(\mathbf{r})$  varies slowly on the scale of the lattice, we replace the sum in Eq. (S24) by an integral:

$$v_0 \sum_k |\phi(\mathbf{R}_k)|^4 \rightarrow \int d^3r |\phi(\mathbf{r})|^4. \quad (\text{S25})$$

Inserting the envelope functions (S2) and (S3) for a quantum dot with height  $a_z$  and radius  $l$  and evaluating the integral in Eq. (S25), we find

$$I_0 = \frac{3}{4} \frac{1}{N}. \quad (\text{S26})$$

Here,  $N$  is the number of nuclear spins within the quantum dot, given explicitly by

$$N = \frac{\pi l^2 a_z}{v_0}. \quad (\text{S27})$$

Inserting Eq. (S26) into Eq. (S23) directly gives Eq. (10) of the main text.

- 
- [S1] R. Winkler, *Spin-Orbit Coupling Effects in Two-Dimensional Electron and Hole Systems*, vol. 191 of *Springer Tracts in Modern Physics* (Springer-Verlag Berlin Heidelberg, 2003), appendix B-D.
- [S2] I. Vurgaftman, J. R. Meyer, and L. R. Ram-Mohan, J. Appl. Phys. **89**, 5815 (2001).
- [S3] D. Paget, G. Lampel, B. Sapoval, and V. I. Safarov, Phys. Rev. B **15**, 5780 (1977).
- [S4] E. Clementi and D. L. Raimondi, J. Chem. Phys. **38**, 2686 (1963).
- [S5] Y. Yafet, J. Phys. Chem. Solids **21**, 99 (1961).
- [S6] D. V. Bulaev and D. Loss, Phys. Rev. Lett. **95**, 076805 (2005).
- [S7] In Winkler's notation [S1], these are the terms proportional to  $C$ ,  $B_{7v}$ , and  $B_{8v}^{\pm}$ . These terms will not lead to considerable corrections for our purposes. However, the terms  $Ck_{\pm}$  could become relevant when considering higher-order effects in the spin-orbit interaction, such as the cubic Dresselhaus terms which were derived in Ref. [S6].